

Characterization and thermal expansion of $\text{Sr}_2\text{Fe}_x\text{Mo}_{2-x}\text{O}_6$ double perovskites

Y MARKANDEYA¹ , Y SURESH REDDY², SHASHIDHAR BALE¹,
C VISHNUVARDHAN REDDY² and G BHIKSHAMAIAH^{2,*}

¹Department of Physics, Nizam College, Osmania University, Hyderabad 500 001, India

²Department of Physics, Osmania University, Hyderabad 500 007, India

MS received 23 February 2015; accepted 25 June 2015

Abstract. Double perovskite oxides $\text{Sr}_2\text{Fe}_x\text{Mo}_{2-x}\text{O}_6$ ($x = 0.8, 1.0, 1.2, 1.3$ and 1.4) (SFMO) of different compositions were prepared by sol–gel growth followed by annealing under reducing atmosphere conditions of H_2/Ar flow. X-ray powder diffraction studies revealed that the crystal structure of the samples changes from tetragonal to cubic at around $x = 1.2$. Lattice parameters and unit cell volume of these samples found to decrease with the increase in Fe content. The characteristics absorption bands observed in the range $400\text{--}1000\text{ cm}^{-1}$ of Fourier transform infrared spectra indicate the presence of FeO_6 and MoO_6 octahedra and confirm the formation of double perovskite phase. The value of $g \sim 2.00$ obtained from electron spin resonance studies indicates that Fe is in $3+$ ionic state in the SFMO samples. Dilatometric studies of these samples reveal that the average value of coefficient of thermal expansion ($\bar{\alpha}$) increases with the increase in temperature or Fe content in SFMO samples. The low value of coefficient of thermal expansion $1.31 \times 10^{-6} \text{ }^\circ\text{C}^{-1}$ obtained for $\text{Sr}_2\text{Fe}_{0.8}\text{Mo}_{1.2}\text{O}_6$ in the present study in the temperature range of $40\text{--}100^\circ\text{C}$ makes it useful as anode material in fuel cells. The coefficient of thermal expansion ($\bar{\alpha}$) and the unit cell volume (V) of SFMO samples vary inversely with composition in agreement with Grüneisen relation.

Keywords. Sol–gel chemistry; oxides; crystal structure; electron microscopy; thermal expansion.

1. Introduction

Double perovskite materials have gained lot of research interest in recent years owing to their significant applications such as anode materials in fuel cells, magnetic storage devices. Especially double perovskite oxide $\text{Sr}_2\text{FeMoO}_6$ doped with several elements were extensively studied for magnetoresistance and magnetization.^{1–17} This compound crystallizes in tetragonal lattice with space group $I4/mmm$.¹ The structure of $\text{Sr}_2\text{FeMoO}_6$ can be viewed as a regular arrangement of corner-sharing FeO_6 and MoO_6 octahedra, alternating along the three directions of the crystal with the Sr cations occupying the voids in between the octahedra.^{1,3} Thermal expansion studies give information regarding the expansion coefficient of a material and its applicability as sealants. However, there is no work reported on thermal expansion studies on these materials except on stoichiometric A_2FeMoO_6 ($A = \text{Sr}, \text{Ba}, \text{Ca}$).¹¹ In addition, Fe and Mo are d-block elements and their ions are of almost same size. In view of this, the authors have taken up synthesis of $\text{Sr}_2\text{Fe}_x\text{Mo}_{2-x}\text{O}_6$ by interchanging Fe and Mo content in their sites with an objective to characterize them using X-ray diffraction (XRD), scanning electron microscopy (SEM), Fourier transform infrared (FTIR) spectroscopy, electron

spin resonance (ESR) and study thermal expansion at elevated temperatures.

2. Experimental

Different composition of $\text{Sr}_2\text{Fe}_x\text{Mo}_{2-x}\text{O}_6$ ($x = 0.8, 1.0, 1.2, 1.3$ and 1.4) (SFMO) powders were synthesized by the sol–gel method using AR grade $\text{Sr}(\text{NO}_3)_2$, $\text{Fe}(\text{NO}_3)_3 \cdot 9\text{H}_2\text{O}$ and H_2MoO_4 . The details of the synthesis of the SFMO powders are given in earlier publications^{7,8} from this laboratory. The powders of SFMO were pressed into pellets of dimensions $25\text{ mm} \times 6\text{ mm} \times 6\text{ mm}$ using a dies under a pressure of 5 t m^{-2} . These pellets were sintered at 1200°C for 6 h and then heated at 1000°C in a stream mixture of gas ($10\% \text{ H}_2 + 90\% \text{ Ar}$) for 3 h for reducing Mo^{6+} into Mo^{5+} . These pellets were subjected to XRD studies using Philips PW 1830 diffractometer with $\text{Cu K}\alpha$ radiation ($40\text{ kV} \times 25\text{ mA}$) to confirm the crystal structure. Surface morphology of the samples was found using the SEM (Model no. Joel JSM-5600) with combined microanalyzer. FTIR spectra of the samples were recorded on Bruker Tensor 27 DTGS TEC detector spectrophotometer in the wavenumber range of $400\text{--}1000\text{ cm}^{-1}$ by the KBr pellet method. ESR spectra were recorded at room temperature using a JOEL-1X-ESR spectrometer that works in X-band frequency range ($8\text{--}12.5\text{ GHz}$) with 100 kHz field modulation. Thermal expansion measurements were performed using Netzsch 402 PC dilatometer in the temperature range of $40\text{--}400^\circ\text{C}$ during heating cycle.

*Author for correspondence (gbhyd08@gmail.com)

3. Result and discussion

3.1 Characterization

XRD patterns of various compositions of SFMO samples are shown in figure 1. These patterns reveal that the observed diffraction profiles belong to double perovskite structure of $\text{Sr}_2\text{Fe}_x\text{Mo}_{2-x}\text{O}_6$.^{4–6} All the profiles of SFMO are indexed and found to be in single phase. The lattice parameters of SFMO were evaluated by Cohen's least square method using (*hkl*) values and Bragg's angles with a suitable computer program. It has been found that SFMO crystallizes in tetragonal lattice (space group *I4/mmm*) for $0.8 \leq x \leq 1.2$ and cubic lattice (space group *Fm3m*) for $x > 1.2$. The values of lattice parameters '*a*' and '*c*' of SFMO are given in table 1. The unit cell volume $V = a^3$ for cubic and $2a^2c$ for tetragonal structure were calculated using lattice parameters and are included in table 1. It is found that the value of '*a*', '*c*' and *V* decreases with the increase of Fe content in both tetragonal and cubic phase. Since the ionic radius of Fe^{3+} (0.645 Å) is larger than that of Mo^{5+} (0.61 Å), the decrease in '*a*', '*c*' and *V* might be attributed to cation or oxygen vacancies or

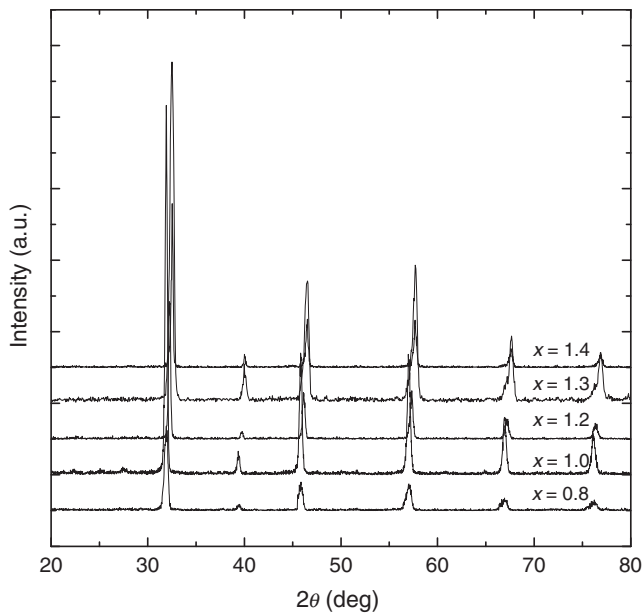


Figure 1. X-ray diffraction patterns of $\text{Sr}_2\text{Fe}_x\text{Mo}_{2-x}\text{O}_6$ ($0.8 \leq x \leq 1.4$) double perovskites recorded at room temperature.

valence disproportion as observed in double perovskites.^{18–20} Further, it can be noted from table 1 that the structural transition from tetragonal to cubic lattice occurs at around $x = 1.2$ in SFMO.²¹ The tolerance factor of SFMO double perovskite is given by

$$t = \frac{r_{\text{Sr}} + r_{\text{O}}}{\sqrt{2} \left(\frac{r_{\text{Fe}}x}{2} + \frac{r_{\text{Mo}}(2-x)}{2} + r_{\text{O}} \right)}, \quad (1)$$

where r_{Sr} , r_{Fe} , r_{Mo} and r_{O} are the ionic radii of Sr, Fe, Mo and O ions, respectively. The tolerance factor (*t*) of SFMO compounds was calculated by employing equation (1) and the values are included in table 1. It is found from table 1 that the deviation of tolerance factor from unity in SFMO samples increases with the increase of Fe content, indicating the increase of distortion from ideal double perovskite structure with Fe content.

The SEM photograph of SFMO sample is shown in figure 2a–e. It is observed from these figures that the porosity is present in the samples. The pore size changes from sample to sample. The pore size is very small and material is closely packed with fewer voids for composition $x = 1.3$. It is slightly larger for rest of the compositions in SFMO samples.

Figure 3 shows FTIR spectra of the $\text{Sr}_2\text{Fe}_x\text{Mo}_{2-x}\text{O}_6$ ($x = 0.8, 1.0, 1.2, 1.3$ and 1.4) samples in the spectral wavenumber range of 400 and 1000 cm^{-1} . Three characteristic absorption bands between 400 and 860 cm^{-1} are usually used to identify the perovskite phase formation.¹² In the present study, FTIR spectra of the SFMO samples show three absorption bands corresponding to Fe–O and Mo–O vibrations, namely, strong bands in the high-wavenumber range ~ 809 and 858 cm^{-1} with associated with the Mo–O symmetric stretching mode of MoO_6 octahedra; broad band at $\sim 630 \text{ cm}^{-1}$ and weak band at $\sim 702 \text{ cm}^{-1}$ assigned to the antisymmetric stretching mode of the MoO_6 octahedra due to the higher charge of this cation.¹³ The weak absorption band obtained at about 422 cm^{-1} is ascribed to Fe–O vibration absorption of FeO_6 octahedra. In SFMO double perovskite samples, the highly charged Mo cation octahedra (MoO_6) acts as independent group, the vibration spectrum therefore arises from such MoO_6 octahedra. Mo–O symmetric stretching mode of MoO_6 octahedra at about 809 and 858 cm^{-1} is usually an infrared inactive vibration, but in a double perovskite, both Fe and Mo ions exist in Fe and Mo sites and it becomes partially allowed due to lowering of site symmetry.¹³

Table 1. Values of lattice parameters (*a* and *c*), unit cell volume (*V*), tolerance factor (*t*) and *g*-factor of the $\text{Sr}_2\text{Fe}_x\text{Mo}_{2-x}\text{O}_6$ ($0.8 \leq x \leq 1.4$) double perovskites.

Composition (<i>x</i>)	0.8	1.0	1.2	1.3	1.4
Lattice parameter (<i>a</i> (Å))	5.574	5.567	5.563	7.839	7.831
Lattice parameter (<i>c</i> (Å))	7.909	7.898	7.889	—	—
Unit cell volume (<i>V</i> (Å ³))	491.46	489.54	488.28	481.70	480.23
Tolerance factor (<i>t</i>)	0.9923	0.9906	0.9889	0.988	0.9872
<i>g</i> -Factor	—	2.045	2.032	2.050	2.024

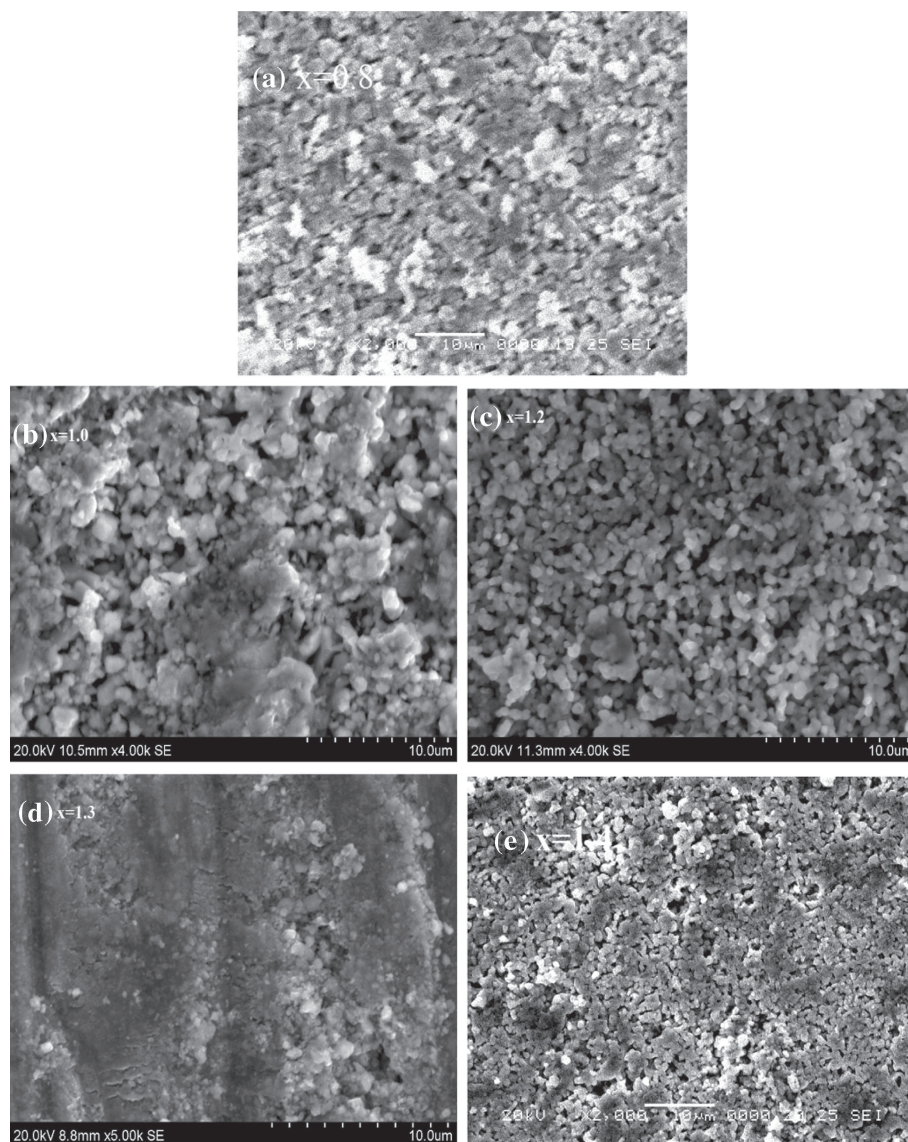


Figure 2. SEM micrographs of $\text{Sr}_2\text{Fe}_x\text{Mo}_{2-x}\text{O}_6$ double perovskites for Fe content (a) $x = 0.8$, (b) $x = 1.0$, (c) $x = 1.2$, (d) $x = 1.3$ and (e) $x = 1.4$.

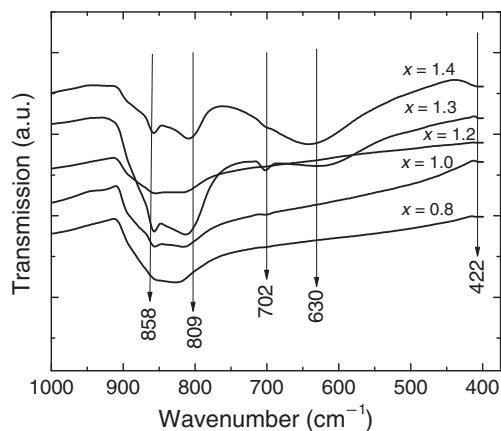


Figure 3. FTIR spectra of $\text{Sr}_2\text{Fe}_x\text{Mo}_{2-x}\text{O}_6$ ($x = 0.8, 1.0, 1.2, 1.3$ and 1.4) samples.

The bands obtained in the present study confirm the formation of perovskite phase.

ESR spectra of $\text{Sr}_2\text{Fe}_x\text{Mo}_{2-x}\text{O}_6$ ($x = 1.0, 1.2, 1.3$ and 1.4) samples taken at room temperature are shown in figure 4a–d. All the figures show a similar spectrum. It is observed from spectra that a peak is resolved at around $H = 310$ mT for all samples. The value of g -factor of SFMO samples were evaluated using $g = h\nu/\beta H$, where h is Planck's constant (6.625×10^{-34} J s), ν the frequency of magnetic field, β the Bohr magneton (9.274×10^{-24} J Tesla $^{-1}$), H the applied magnetic field. The value of g -factor thus obtained is included in table 1. It is found from table 1 that the value of g -factor is close to 2.00, indicating Fe is in 3+ state in SFMO samples. Therefore, the ESR spectra of SFMO samples obtained in this study correspond to the localized 3d 5 Fe cores in the band picture as reported by Kobayashi *et al.*¹ This rules out the possibility of assigning the observed spin

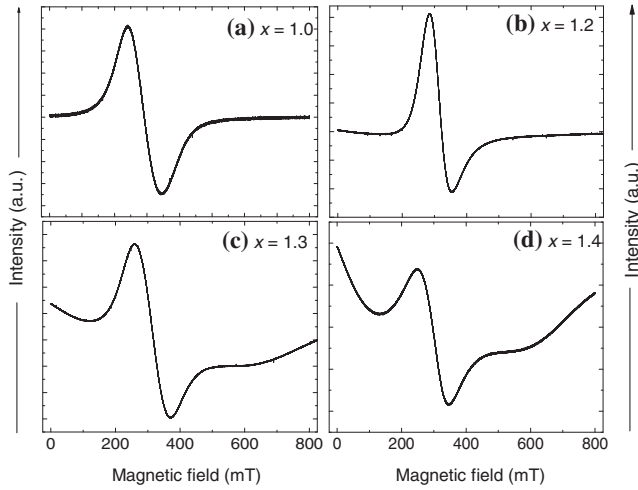


Figure 4. ESR spectrum of $\text{Sr}_2\text{Fe}_x\text{Mo}_{2-x}\text{O}_6$ samples for (a) $x = 1.0$, (b) $x = 1.2$, (c) $x = 1.3$ and (d) $x = 1.4$.

resonance to localized Fe^{2+} in SFMO samples. Because its ground state in octahedral environment is a triplet with an expected g -factor about 3.4. On the other hand, if Fe^{2+} ions were also present, their short relaxation time would render their ESR line undetectable as in the case of FeO. If this was the case, the Fe^{2+} – Fe^{3+} coupling would induce a g -shift to the Fe^{3+} ESR line.¹⁴ Hence, in the present study, it can be concluded that SFMO samples contain Fe^{3+} ions only since the observed g -value remains constant in the whole composition range. Further, the small distortion observed in the shape of spectrum for the samples $x > 1.2$ in figure 4c and d might be attributed to structural phase change from tetragonal to cubic at $x = 1.2$ in conformity with results obtained from XRD studies.

3.2 Thermal expansion

The thermal expansion characteristics ($\Delta L/L_0$) of $\text{Sr}_2\text{Fe}_x\text{Mo}_{2-x}\text{O}_6$ ($x = 0.8, 1.0, 1.2, 1.3$ and 1.4) in the temperature range from 40 to 400°C obtained using dilatometer are shown in figure 5. The thermal expansion depends on the electrostatic forces within the lattice, which depend on the concentration of positive and negative charges and their distances within the lattice.²² The thermal expansion of a solid is characterized by the coefficient of thermal expansion (α) caused by the thermal lattice vibrations given by

$$\alpha = \frac{d}{dT} \left(\frac{\Delta L}{L_0} \right) = \frac{L_1 - L_0}{L_0(T_1 - T_0)}, \quad (2)$$

where L_0 and L_1 are the lengths of sample at temperature T_0 and T_1 , respectively.

The experimental data of thermal expansion ($\Delta L/L_0$) as a function of temperature (T) of SFMO samples in the present study can be fitted to a polynomial of degree 2 as

$$\frac{\Delta L}{L_0} = A + BT + CT^2, \quad (3)$$

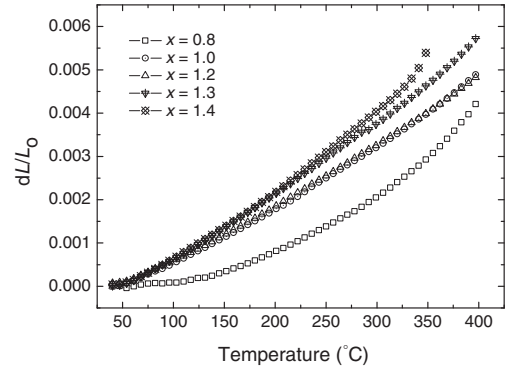


Figure 5. Variation of $\Delta L/L_0$ as a function of temperature of $\text{Sr}_2\text{Fe}_x\text{Mo}_{2-x}\text{O}_6$ ($0.8 \leq x \leq 1.4$) double perovskites.

where A , B and C are the constants and given in table 2 for all the samples. The value of α then can be determined using the first derivative of equation (3) with respect to temperature as

$$\alpha = \frac{d}{dT} \left(\frac{\Delta L}{L_0} \right) = B + 2CT, \quad (4)$$

Equation (4) shows that the value of α at any temperature can be obtained using constants B and C .

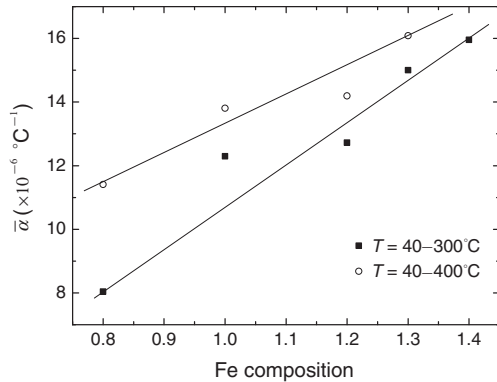
The average value of coefficient of thermal expansion ($\bar{\alpha}$) in the temperature range from T_0 to T_1 can be determined using the relation

$$\bar{\alpha} = \frac{1}{T_1 - T_0} \int_{T_0}^{T_1} (B + 2CT) dT. \quad (5)$$

Thus, the value of $\bar{\alpha}$ was evaluated in different temperature ranges namely 40–100, 40–200, 40–300 and 40–400°C for all SFMO materials and are given in table 2. The plot of $\bar{\alpha}$ vs. Fe composition of SFMO in the temperature ranges 40–300 and 40–400°C is shown in figure 6 and it is observed that the value of $\bar{\alpha}$ increases with the Fe content and temperature. Falcon *et al*²³ investigated the oxidation profiles of $\text{Sr}_2\text{FeMoO}_{6-\delta}$ oxide, results showed that oxygen was relatively easily incorporated into the perovskite structure. Increase in the oxygen vacancy concentration leads to oxygen permeation and lattice expansion which becomes much more pronounced.²⁴ Therefore, in the present study increase in the value of $\bar{\alpha}$ of SFMO samples with the increase in temperature may be attributed to increase in concentration of oxygen vacancy. Zhang *et al*¹¹ have reported that the value of $\bar{\alpha}$ of $\text{Sr}_2\text{FeMoO}_{6-\delta}$ in the temperature range 30–1000°C is $13.9 \times 10^{-6} \text{ } ^\circ\text{C}^{-1}$. The value of $\bar{\alpha}$ of $\text{Sr}_2\text{FeMoO}_6$ obtained in the present study in the temperature ranges 40–400 °C^{−1} is $13.8 \times 10^{-6} \text{ } ^\circ\text{C}^{-1}$ is very much in agreement with that reported by Zhang *et al*.¹¹ It is also found from figure 6 that the value of $\bar{\alpha}$ increases with the increase in Fe content. This increase in $\bar{\alpha}$ may be attributed to substitution of larger ionic size of Fe^{3+} (0.645 Å) at smaller ionic size of Mo^{5+} site (0.61 Å). Further, it is to be noted that the average value of coefficient of thermal expansion of $\text{Sr}_2\text{Fe}_{0.8}\text{Mo}_{1.2}\text{O}_6$ is found to be

Tabl Values of constants A , B , C of equation (3), and average value of coefficient of thermal expansion ($\bar{\alpha}$) in different temperature ranges for $\text{Sr}_2\text{Fe}_x\text{Mo}_{2-x}\text{O}_6$ ($0.8 \leq x \leq 1.4$) double perovskites.

Composition (x)	A	B	C	$\bar{\alpha} (\times 10^{-6} \text{ }^\circ\text{C}^{-1})$			
				40–100°C	40–200°C	40–300°C	40–400°C
0.8	0.99×10^{-4}	-3.41×10^{-6}	3.37×10^{-8}	1.31	4.67	8.01	11.41
1.0	-4.31×10^{-4}	8.70×10^{-6}	1.16×10^{-8}	10.32	11.48	12.29	13.80
1.2	-4.44×10^{-4}	9.61×10^{-6}	0.91×10^{-8}	10.88	11.79	12.72	14.19
1.3	-5.81×10^{-4}	11.33×10^{-6}	1.08×10^{-8}	12.83	13.92	15.00	16.08
1.4	-4.45×10^{-4}	8.95×10^{-6}	2.06×10^{-8}	11.83	13.89	15.95	—



Fi Variation of average value of coefficient of thermal expansion ($\bar{\alpha}$) with Fe composition at different temperature ranges 40–300 and 40–400°C of SFMO samples.

$1.31 \times 10^{-6} \text{ }^\circ\text{C}^{-1}$ in the temperature range 40–100°C makes this material in fuel cell applications as anodes.

It is observed from table 1 and figure 6 that the value of unit cell parameters decrease and the value of $\bar{\alpha}$ increases with the increase in Fe content, indicating an inverse relation between the value of $\bar{\alpha}$ and unit cell parameters in accordance with the following Gruneisen's relation:^{22,25}

$$\alpha_v = \frac{\gamma_G C_v \chi}{V}, \quad (6)$$

where α_v is the coefficient of volume thermal expansion, γ_G Gruneisen's constant, C_v the heat capacity at constant volume, χ the compressibility, and V the volume of the unit cell.

4.

- (1) It has been found that the lattice parameters and unit cell volume decreases with the increase of Fe content in SFMO samples.
- (2) A structural transition from tetragonal to cubic at around $x = 1.2$ is observed in SFMO samples.
- (3) The FTIR spectra of SFMO showed three characteristic absorption bands in the range of 860–400 cm^{-1} , indicating the formation of perovskite structure.
- (4) ESR results of the samples show that the iron is in Fe^{3+} state in SFMO samples.

- (5) The results of thermal expansion showed that the average value of coefficient of thermal expansion ($\bar{\alpha}$) increases with the increase in temperature or Fe content in SFMO samples.

Acknowledgements

One of the authors (GB) wish to thank DST for providing financial assistance to carry out this work through a project OU-DST-PURSE-Scheme No. A.60. We express our gratitude to the Head, Department of Physics, Osmania University and the Head, Department of Physics and Principal, Nizam College, Osmania University, Hyderabad, for their encouragement. We also thank Prof V Seshubai, University of Hyderabad, for providing ESR measurements.

References

1. Kobayashi K I, Kimura T, Sawada H, Terakura K and Tokura Y 1998 *Nature (Lond.)* **395** 677
2. Ray S, Middey S, Jana S, Banerjee A, Sanyal P, Rawat R, Gregoratti L and Sarma D D 2011 *J. EPL* **94** 47007
3. Lu M F, Wang J P, Liu J F, Song W, Hao X F, Zhou D F, Liu X J, Wu Z J and Meng J 2007 *J. Alloys Compd.* **428** 214
4. Gaur A, Varma G D and Singh H K 2008 *J. Alloys Compd.* **460** 581
5. Bufaiçal L, Adriano C, Lora-Serrano R, Duque J G S, Mendonça-Ferreira L, Rojas-Ayala C, Baggio-Saitovitch E, Bittar E M and Pagliuso P G 2014 *J. Solid State Chem.* **212** 23
6. Feng X M, Rao G H, Liu G Y, Yang H F, Liu W F, Ouyang Z W and Liang J K 2004 *Physica B* **344** 21
7. Markandeya Y, Suresh K and Bhikshamaiah G 2011 *J. Alloys Compd.* **509** 9598
8. Markandeya Y, Saritha D, Vithal M, Singh A K and Bhikshamaiah G 2011 *J. Alloys Compd.* **509** 5195
9. Huo G, Ren X, Qian L, Zhang N, Liu S and Yan X 2013 *J. Magn. Magn. Mater.* **343** 119
10. Mohamed Musa Saad H-E 2012 *Physica B* **407** 2512
11. Zhang L, Zhou Q, He Q and He T 2010 *J. Power Sources* **195** 6356
12. Mostafa M F, Ata-Allah S S, Youssef A A A and Refai H S 2008 *J. Magn. Magn. Mater.* **320** 344
13. Lavat A E and Baran E J 2003 *Vib. Spectrosc.* **32** 167

14. Gulley J E and Jaccarino V 1972 *Phys. Rev. B* **6** 58
15. Kapusta Cz, Riedi P C, Zajac D, Sikora M, De Teresa J M, Morellon L and Ibarra M R 2002 *J. Magn. Magn. Mater.* **242–245** 701
16. Kim S B, Lee B W and Kim C S 2002 *J. Magn. Magn. Mater.* **242–245** 747
17. Xue J, Shen Y and He T 2011 *J. Power Sources* **196** 3729
18. Topfer J and Goodenough J B 1997 *Chem. Mater.* **9** 1467
19. van Roosmalen J A M, van Vlaanderen P, Cordfunke E H P, Ijdo W L and Ijdo D J W 1995 *J. Solid State Chem.* **114** 516
20. Takeda Y, Kanno K, Takada T, Yamamoto O, Takano M, Nakayama N and Bando Y 1986 *J. Solid State Chem.* **63** 237
21. Yoshida K, Keuchi S I, Shimizu H, Okayasu S and Suzuki T 2011 *J. Phys. Soc. Jpn.* **80** 044716
22. Prasanth Kumar V, Reddy Y S, Kistaiah P, Prasad G and Vishnuvardhan Reddy C 2008 *Mater. Chem. Phys.* **112** 711
23. Falcon H, Barbero J A, Araujo G, Casais M T, Martinez-Lope M J, Alonso J A and Fierro J L G 2004 *Appl. Catal. B—Environ.* **53** 37
24. Onuma S, Yashiro K, Miyoshi S, Kaimai A, Matsumoto H, Nigara Y, Kawada T, Mizusaki J, Kawamura K, Sakai N and Yokokawa H 2004 *Solid State Ion.* **174** 287
25. Eastabrook J N 1957 *Philos. Mag.* **2** 1421